

Accepted Manuscript

Molecular structure, FT-IR, first order hyperpolarizability, NBO analysis, HOMO and LUMO, MEP analysis of (*E*)-3-(4-chlorophenyl)-1-(4-fluorophenyl)prop-2-en-1-one by HF and density functional methods

A. Najiya, C. Yohannan Panicker, M. Sapnakumari, B. Narayana, B.K. Sarojini, C. Van Alsenoy

PII: S1386-1425(14)00937-8
DOI: <http://dx.doi.org/10.1016/j.saa.2014.06.049>
Reference: SAA 12308

To appear in: *Spectrochimica Acta Part A: Molecular and Biomolecular Spectroscopy*

Received Date: 23 April 2014
Revised Date: 17 May 2014
Accepted Date: 3 June 2014

Please cite this article as: A. Najiya, C. Yohannan Panicker, M. Sapnakumari, B. Narayana, B.K. Sarojini, C. Van Alsenoy, Molecular structure, FT-IR, first order hyperpolarizability, NBO analysis, HOMO and LUMO, MEP analysis of (*E*)-3-(4-chlorophenyl)-1-(4-fluorophenyl)prop-2-en-1-one by HF and density functional methods, *Spectrochimica Acta Part A: Molecular and Biomolecular Spectroscopy* (2014), doi: <http://dx.doi.org/10.1016/j.saa.2014.06.049>

This is a PDF file of an unedited manuscript that has been accepted for publication. As a service to our customers we are providing this early version of the manuscript. The manuscript will undergo copyediting, typesetting, and review of the resulting proof before it is published in its final form. Please note that during the production process errors may be discovered which could affect the content, and all legal disclaimers that apply to the journal pertain.



Molecular structure, FT-IR, first order hyperpolarizability, NBO analysis, HOMO and LUMO, MEP analysis of (*E*)-3-(4-chlorophenyl)-1-(4-fluorophenyl)prop-2-en-1-one by HF and density functional methods

A.Najiya^a, C.Yohannan Panicker^{a*}, M. Sapnakumari^b, B.Narayana^b, B.K.Sarojini^c, C.Van Alsenoy^d

^aDepartment of Physics, TKM College of Arts and Science, Kollam, Kerala, India.

^bDepartment of Studies in Chemistry, Mangalore University, Mangalagangothri, Karnataka, India.

^cIndustrial Chemistry-Division, Department of Studies in Chemistry, Mangalore University, Mangalagangothri, Karnataka, India.

^dDepartment of Chemistry, University of Antwerp, B2610 Antwerp, Belgium.

Author for correspondence: email: cyphyp@rediffmail.com

Phone : +91 9895370968

Abstract

(*E*)-3-(4-chlorophenyl)-1-(4-fluorophenyl)prop-2-en-1-one is synthesized by reacting 4-fluoroacetophenone and 4-chlorobenzaldehyde in ethanol and sodium hydroxide solution. The structure of the compound was confirmed by IR and single crystal X-ray diffraction studies. FT-IR spectrum of (*E*)-3-(4-chlorophenyl)-1-(4-fluorophenyl)prop-2-en-1-one was recorded and analyzed. The crystal structure is also described. The vibrational wavenumbers were calculated using HF and DFT methods and are assigned with the help of potential energy distribution method. The geometrical parameters of the title compound obtained from XRD studies are in agreement with the calculated (DFT) values. The stability of the molecule arising from hyper-conjugative interaction and charge delocalization has been analyzed using NBO analysis. The calculated first hyperpolarizability of the title compound is comparable with the reported values of similar derivatives and 63.85 times that of the standard NLO material urea. The HOMO-LUMO transition implies an electron density transfer from the chlorophenyl ring to the fluorophenyl ring. From the MEP analysis it is evident that the negative charge covers the C=O group and the positive region is over the phenyl rings.

Keywords: Chlorophenyl; Fluorophenyl; FT-IR; Hyperpolarizability; MEP.

1. Introduction

Chalcone (1,3-diphenyl-2-propene-1-one) and related compounds “chalconoids” are those in which two aromatic rings are linked and conjugated together through a reactive keto ethylenic linkage (-CO-CH=CH-), which impart an entirely delocalized π -electron system on both benzene rings in such a way that this system has relatively low redox potentials and has a greater probability of undergoing electron transfer reaction [1]. Chalcones with their unique chemical structure will display a wide range of pharmacological activities depending on the nature, number and position of the substituents on both benzene rings of the structure. Chalcones are well known intermediates for synthesizing various heterocyclic compounds. The compounds with the backbone of chalcones have been reported to possess various biological activities such as antimicrobial [2], anti-inflammatory [3], analgesic [4], anti-platelet [5], anti-ulcerative [6], anti-malarial [7], anticancer [8], antiviral [9], antileishmanial [10], antioxidant [11], antitubercular [12], antihyperglycemic [13], immunomodulatory [14], inhibition of chemical mediators release [15], inhibition of leukotriene B4 [16], inhibition of tyrosinase [17] and inhibition of aldose reductase activities [18]. Additionally, some of the chalcone derivatives have been found to inhibit several important enzymes in cellular systems, such as xanthine oxidase, mammalian α -amylase, cyclooxygenase, 5-lipoxygenase, while others demonstrated the ability to block voltage dependent potassium and calcium channels [19-20]. In the present study, IR spectrum of (*E*)-3-(4-chlorophenyl)-1-(4-fluorophenyl)prop-2-en-1-one was reported both experimentally and theoretically. The energies, degrees of hybridization, populations of the lone pairs of oxygen, chlorine, fluorine, energies of their interaction with the anti-bonding orbital of the phenyl ring and the electron density distribution and E(2) energies have been calculated by NBO analysis using DFT method to give clear evidence of stabilization originating from the hyper-conjugation of various intra-molecular interactions. There has been growing interest in using organic materials for nonlinear optical devices, functioning as second harmonic generators, frequency converters, electro-optical modulators, etc., because of the large second order electric susceptibilities of organic materials. Since the second order electric susceptibility is related to the first hyperpolarizability, the search for organic chromophores with large first hyperpolarizability is fully justified.

2. Experimental

To a mixture of 4-fluoroacetophenone (1.38gm, 0.01mol) and 4-chlorobenzaldehyde (1.41g, 0.01mol) in ethanol (100ml), 15 ml of 10% sodium hydroxide solution was added and stirred at 0-5°C for 3h. The precipitate formed was collected by filtration and purified by re-crystallization from ethanol. Colorless blocks were grown from toluene as solvent by the slow evaporation method. A Bruker APEX2 CCD diffractometer equipped with graphite monochromator Mo $k\alpha$ ($\lambda = 0.71073\text{\AA}$) radiation was used for the measurement of data. The collected data were reduced using the SAINT program and structural refinement was carried out by full matrix least squares on F^2 (SHELXL-97) program package [21]. Molecular graphic employed includes ORTEP 3 and Mercury. The ORTEP diagram and crystal packing are given in Figs. S1 and S2 as supporting material. In the title compound, $C_{15}H_{10}ClFO$, the fluoro substituted benzene ring forms a dihedral angle of 44.4° with the chloro substituted benzene ring. The only significant directional bonds in the crystal are weak C-H... π interactions. FT-IR spectrum (Fig. 1) was recorded using KBr pellets on a Shimadzu-FTIR infrared spectrometer.

3. Computational details

Calculations of the title compound are carried out with Gaussian09 program [22] using the HF/6-31G(6D,7F) and B3LYP/6-31G(6D,7F) basis sets to predict the molecular structure and vibrational wavenumbers. Molecular geometry was fully optimized by Berny's optimization algorithm using redundant internal coordinates. Harmonic vibrational wavenumbers were calculated using the analytic second derivatives to confirm the convergence to minima on the potential surface. The DFT hybrid B3LYP functional method tends to overestimate the fundamental modes; therefore scaling factor of 0.9613 has to be used for obtaining a considerably better agreement with experimental data [23]. For HF method a scaling factor of 0.8929 is used [23]. Parameters corresponding to optimized geometry (B3LYP) of the title compound with experimental data (Fig. 2) are given in Table S1(supporting material). The absence of imaginary wavenumbers on the calculated vibrational spectrum confirms that the structure deduced corresponds to minimum energy. The assignments of the calculated wave numbers are aided by the animation option of GAUSSVIEW program, which gives a visual

presentation of the vibrational modes [24]. The potential energy distribution (PED) is calculated with the help of GAR2PED software package [25].

4. Results and discussion

4.1. IR spectrum

The calculated (scaled wavenumbers), observed IR bands and assignments are given in Table 1. In the following discussion, the phenyl rings attached with the chlorine and fluorine atoms are designated as PhI and PhII respectively. The existence of one or more aromatic rings in a structure is normally readily determined from the C=C-C ring related modes and C-H vibrations. The C-H stretching modes occurs above 3000 cm^{-1} and is typically exhibited as a multiplicity of weak to moderate bands, compared with the aliphatic C-H stretch [26]. For the title compound, CH stretching vibrations of the phenyl rings are assigned in the range $3073\text{-}3103\text{ cm}^{-1}$ for PhI and $3096\text{-}3110\text{ cm}^{-1}$ for PhII theoretically. The benzene ring possesses six ring stretching vibrations, of which the four with the highest wavenumbers (occurring near 1600 , 1580 , 1490 and 1440 cm^{-1}) are good group vibrations [27]. With heavy substituents, the bands tend to shift to somewhat lower wavenumbers. In the absence of ring conjugation, the band at 1580 cm^{-1} is usually weaker than that at 1600 cm^{-1} . In the case of C=O substitution, the band near 1490 cm^{-1} can be very weak. The fifth ring stretching vibration is active near $1315 \pm 65\text{ cm}^{-1}$, a region that overlaps strongly with that of the CH in-plane deformation. The sixth ring stretching vibration, or the ring breathing mode, appears as a weak band near 1000 cm^{-1} in mono-, 1,3-di-, and 1,3,5-trisubstituted benzenes [27]. In the otherwise substituted benzenes, however, this vibration is substituent sensitive and difficult to distinguish from the ring in-plane deformation [27]. The ν_{Ph} modes are expected in the region $1280\text{-}1630\text{ cm}^{-1}$ for para-substituted phenyl rings [27] and the modes observed 1551 , 1279 cm^{-1} and 1496 , 1402 cm^{-1} in the IR spectrum are assigned as the phenyl ring CC stretching modes for PhI and PhII. The DFT calculations give these modes at 1584 , 1552 , 1480 , 1395 , 1276 cm^{-1} for PhI and 1596 , 1573 , 1497 , 1400 , 1305 cm^{-1} for PhII. The ring breathing mode of the para-disubstituted benzenes with entirely different substituents [28] has been reported in the interval $780\text{-}880\text{ cm}^{-1}$. For the title compound, this is confirmed by the bands in the infrared spectrum at 820 , 878 cm^{-1} and at 817 , 874 cm^{-1} theoretically, which finds support from computational results. For para substituted benzene, the ring breathing

mode is reported at 873 cm^{-1} in IR spectrum and 861 cm^{-1} theoretically [29]. The in-plane CH deformation bands of the phenyl ring are expected above 1000 cm^{-1} [27] and in the present case, the bands at 1098 cm^{-1} (IR), 1286, 1169, 1099, 1070 cm^{-1} (DFT) and 1148, 1007 cm^{-1} (IR), 1272, 1144, 1088, 1007 cm^{-1} (DFT) are assigned as the in-plane CH deformation for PhI and PhII respectively. The CH out-of-plane deformations of the phenyl ring [27] are observed between 1000 and 700 cm^{-1} . Generally, the CH out-of-plane deformations with the highest wavenumbers have weaker intensity than those absorbing at lower wavenumbers. The bands observed at 952, 820, 806, 790 cm^{-1} in IR spectrum are assigned as the CH out-of-plane deformations of the phenyl rings. The corresponding theoretical values are 928, 923, 804, 801 cm^{-1} for PhI and 954, 909, 827, 794 cm^{-1} for PhII. The strong γCH occurring at $840 \pm 50\text{ cm}^{-1}$, is typical for 1,4-disubstitution, and the bands observed at 806, 820 cm^{-1} in the IR spectrum is assigned to this mode. The B3LYP calculations give these modes at 804, 827 cm^{-1} . The IR bands in the $1800\text{-}2900\text{ cm}^{-1}$ region and their large broadening support the intra molecular hydrogen bonding [30].

Fluorine atoms directly attached to the aromatic ring give rise bands [31] in the region $1100\text{-}1270\text{ cm}^{-1}$. Many of these compounds [31] including one fluorine atom only on the ring absorb near 1230 cm^{-1} . The $\nu\text{C-F}$ is reported at 1157, 1233 cm^{-1} (IR), 1244 cm^{-1} (HF) [32]. For the title compound, the DFT calculations give CF stretching mode at 1239 cm^{-1} . The vibrations belonging to the bond between the ring and chlorine atoms are worth to discuss here since mixing of vibrations is possible due to the lowering of the molecular symmetry and the presence of heavy atoms on the periphery of the molecule [33]. Mooney [34, 35] assigned vibrations of C-Cl, Br, and I in the wavenumber range of $1129\text{-}480\text{ cm}^{-1}$. The CCl stretching vibrations give generally strong bands in the region $710\text{-}505\text{ cm}^{-1}$. For simple organic chlorine compounds, CCl absorptions are in the region $750\text{-}700\text{ cm}^{-1}$. Sundaraganesan *et al.* [36] reported CCl stretching at 704 (IR), 705 (Raman), and 715 cm^{-1} (DFT) and the deformation bands at 250 and 160 cm^{-1} . The aliphatic CCl absorb [27] in the range $830\text{-}560\text{ cm}^{-1}$ and putting more than one chlorine atom on a carbon atom raises the CCl wavenumber. Pazdera *et al.* [37, 38] reported the CCl stretching mode at 890 cm^{-1} . For 2-cyanophenylisocyanide dichloride, the CCl stretching mode is reported at 870 (IR), 877 (Raman), and 882 cm^{-1} theoretically [39].

For the title compound, the band observed at 645 cm^{-1} in the IR spectrum and 648 cm^{-1} (DFT) is assigned as the CCl stretching mode. The deformation bands of CCl are also identified. This is in agreement with the literature data [40, 41]. For 4-chlorophenylboronic acid, the CCl stretching and deformation bands are reported at 571 cm^{-1} (DFT), and at 287 and 236 cm^{-1} , respectively [42].

The appearance of strong bands in the IR spectrum (less polarizability resulting due to highly dipolar carbonyl bond) in aromatic compounds is the salient feature of the presence of carbonyl group and are due to the C=O stretching motions. The wavenumber of the C=O stretch due to the carbonyl group mainly depends on the bond strength, which in turn depends upon inductive, conjugative, steric effects and lone pair of electron on oxygen. The carbonyl stretching C=O vibration [27, 31, 43] is expected in the region $1750\text{-}1680\text{ cm}^{-1}$ and in the present case this mode appears at 1665 cm^{-1} in the IR spectrum and the DFT calculation gives this mode at 1676 cm^{-1} . The in-plane and out-of-plane C=O deformations are expected in the regions 625 ± 70 and $540 \pm 80\text{ cm}^{-1}$, respectively [27]. The $\delta\text{C=O}$ in-plane deformation band is assigned at 767 cm^{-1} theoretically (DFT). The band observed at 586 cm^{-1} in the IR spectrum and at 581 cm^{-1} (DFT) is assigned as $\gamma\text{C=O}$ mode. Cinar and Karabacak [44] reported the bands at 1697 cm^{-1} in IR, 1700 cm^{-1} in Raman and 1684 cm^{-1} (theoretical) as C=O stretching mode. Arjunan et al. [45] reported C=O modes at $1776, 1716, 864, 723\text{ cm}^{-1}$ in IR spectrum for an anhydride derivative. Mariappan and Sundaraganesan [46] reported 1760 cm^{-1} in the IR spectrum and 1764 cm^{-1} in the Raman spectrum as C=O stretching mode for phenyl carbonate derivative. The C=C stretching mode is expected in the region [43] $1667\text{-}1640\text{ cm}^{-1}$. According to Socrates [47] the C=C stretching mode is expected around 1600 cm^{-1} when conjugated with C=O group. For the title compound, the C=C stretching mode is assigned at 1605 cm^{-1} in the IR spectrum and at 1604 cm^{-1} theoretically. For a series of propenoic acid esters, Felfoldi et al. [48] reported $\nu\text{C=O}$ at 1690 cm^{-1} and $\nu\text{C=C}$ at 1625 cm^{-1} . For the title compound, the CH modes associated with the anhydride group are assigned at 1330 cm^{-1} (in-plane bending), 858 cm^{-1} (out-of-plane bending) in the IR spectrum and at $3053, 3085\text{ cm}^{-1}$ (stretching modes), $1324, 1315\text{ cm}^{-1}$ (in-plane bending), $999, 856\text{ cm}^{-1}$ (out-of-plane bending) theoretically (DFT). The substituent sensitive modes

of the phenyl ring and other modes are also identified and assigned (Table 1). Most of the modes are not pure but contains significant contributions from other modes also.

In order to investigate the performance of vibrational wavenumbers of the title compound the root mean square (RMS) value between the calculated and observed wavenumbers were calculated. The RMS values of wavenumbers were calculated using the following expression [49].

$$RMS = \sqrt{\frac{1}{n-1} \sum_i^n (v_i^{calc} - v_i^{exp})^2} .$$

The RMS errors of the observed IR bands are found to be 38.13 for HF and 10.62 for DFT methods. The small differences between experimental and calculated vibrational modes are observed. This is due to the fact that experimental results belong to solid phase and theoretical calculations belong to gaseous phase.

4.2. NLO properties

Nonlinear optics deals with the interaction of applied electromagnetic fields in various materials to generate new electromagnetic fields, altered in wavenumber, phase, or other physical properties [50]. Organic molecules able to manipulate photonic signals efficiently are of importance in technologies such as optical communication, optical computing, and dynamic image processing [51, 52]. In this context, the dynamic first hyperpolarizability of the title compound is also calculated in the present study. The first hyperpolarizability (β_0) of this novel molecular system is calculated using DFT method, based on the finite field approach. In the presence of an applied electric field, the energy of a system is a function of the electric field. First hyperpolarizability is a third rank tensor that can be described by a $3 \times 3 \times 3$ matrix. The 27 components of the 3D matrix can be reduced to 10 components due to the Kleinman symmetry [53]. The components of β are defined as the coefficients in the Taylor series expansion of the energy in the external electric field. When the electric field is weak and homogeneous, this expansion becomes

$$E = E_0 - \sum_i \mu_i F^i - \frac{1}{2} \sum_{ij} \alpha_{ij} F^i F^j - \frac{1}{6} \sum_{ijk} \beta_{ijk} F^i F^j F^k - \frac{1}{24} \sum_{ijkl} \gamma_{ijkl} F^i F^j F^k F^l + \dots$$

where E_0 is the energy of the unperturbed molecule, F_i is the field at the origin, μ_i , α_{ij} , β_{ijk} and γ_{ijkl} are the components of dipole moment, polarizability, the first hyperpolarizabilities, and second hyperpolarizabilities, respectively. The calculated first

hyperpolarizability of the title compound is 8.30×10^{-30} esu, which is comparable with the reported values of similar derivatives [49]. The calculated hyperpolarizability of the title compound is 63.85 times that of the standard NLO material urea (0.13×10^{-30} esu) [54]. We conclude that the title compound is an attractive object for future studies of nonlinear optical properties.

4.3. NBO analysis

The natural bond orbitals (NBO) calculations were performed using NBO 3.1 program [55] as implemented in the Gaussian09 package at the B3LYP/6-31G* level in order to understand various second-order interactions between the filled orbitals of one subsystem and vacant orbitals of another subsystem, which is a measure of the intermolecular delocalization or hyper conjugation. NBO analysis provides the most accurate possible 'natural Lewis structure' picture of 'j' because all orbital details are mathematically chosen to include the highest possible percentage of the electron density. A useful aspect of the NBO method is that it gives information about interactions of both filled and virtual orbital spaces that could enhance the analysis of intra and inter molecular interactions. The second-order Fock-matrix was carried out to evaluate the donor-acceptor interactions in the NBO basis. The interactions result in a loss of occupancy from the localized NBO of the idealized Lewis structure into an empty non-Lewis orbital. For each donor (i) and acceptor (j) the stabilization energy (E2) associated with the delocalization $i \rightarrow j$ is determined as

$$E(2) = \Delta E_{ij} = q_i \frac{(F_{i,j})^2}{(E_j - E_i)}$$

$q_i \rightarrow$ donor orbital occupancy, $E_i, E_j \rightarrow$ diagonal elements, $F_{ij} \rightarrow$ the off diagonal NBO Fock matrix element.

In NBO analysis large E(2) value shows the intensive interaction between electron-donors and electron-acceptors and greater the extent of conjugation of the whole system, the possible intensive interactions are given in Table S2 (supporting material). The second-order perturbation theory analysis of Fock matrix in NBO basis shows strong intra-molecular hyper-conjugative interactions of π -electrons. The intra-molecular hyper-conjugative interactions are formed by the orbital overlap between $n(\text{Cl})$ and $\pi^*(\text{C-C})$ bond orbital which results in ICT causing stabilization of the system. The strong

intramolecular hyper-conjugative interaction of C₂₂-C₂₄ from Cl₁ of n₃(Cl₁)→π*(C₂₂-C₂₄) which increases ED (0.38533e) that weakens the respective bonds leading to stabilization of 12.46 kcalmol⁻¹. Another intra-molecular hyper-conjugative interactions are formed by the orbital overlap between n(O) and σ*(C-C) bond orbital which results in ICT causing stabilization of the system. The strong intra-molecular hyper-conjugative interaction of C₁₃-C₁₄ from O₂ of n₂(O₃)→σ*(C₁₃-C₁₄) which increases ED (0.06394e) that weakens the respective bonds leading to stabilization of 19.36 kcalmol⁻¹. The strong intra-molecular hyper-conjugative interaction of C₆-C₈ from F₂ of n₃(F₂)→π*(C₆-C₈) which increases ED (0.37043e) that weakens the respective bonds leading to stabilization of 21.05 kcalmol⁻¹.

The increased electron density at the oxygen, chlorine, fluorine atoms leads to the elongation of respective bond length and a lowering of the corresponding stretching wavenumber. The electron density (ED) is transferred from the n(Cl) to the anti-bonding π* orbital of the C-C, n(O) to σ*(C-C), and n(F) to π*(C-C) explaining both the elongation and the red shift [56]. The C-Cl, -C=O, -C-F stretching modes can be used as a good probe for evaluating the bonding configuration around the corresponding atoms and the electronic distribution of the benzene molecule. Hence the title compound is stabilized by these orbital interactions.

The NBO analysis also describes the bonding in terms of the natural hybrid orbital n₂(Cl₁), which occupy a higher energy orbital (-0.32655a.u.) with considerable p-character (100%) and low occupation number (1.97275a.u.) and the other n₁(Cl₁) occupy a lower energy orbital (-0.92528a.u.) with p-character (17.71%) and high occupation number (1.99331a.u.). Also n₂(F₂), which occupy a higher energy orbital (-0.41098a.u.) with considerable p-character (100.0%) and low occupation number (1.96810a.u.) and the other n₁(F₂) occupy a lower energy orbital (-1.0287a.u.) with p-character (30.81%) and high occupation number (1.98843a.u.). n₂(O₃), which occupy a higher energy orbital (-0.25097a.u.) with considerable p-character (100.0%) and low occupation number (1.88470a.u.) and the other n₁(O₃) occupy a lower energy orbital (-0.67888a.u.) with p-character (41.88%) and high occupation number (1.97832a.u.). Thus, a very close to pure p-type lone pair orbital participates in the electron donation to the π*(C-C) orbital for

$n3(\text{Cl}_2) \rightarrow \pi^*(\text{C}-\text{C})$ and $n3(\text{F}_2) \rightarrow \pi^*(\text{C}-\text{C})$, $\sigma^*(\text{C}-\text{C})$ orbital for $n(\text{O}) \rightarrow \sigma^*(\text{C}-\text{C})$ interactions in the compound. The results are given in table S3 as supporting material.

4.4 Frontier molecular orbitals

Frontier molecular orbital refer to the highest occupied molecular orbital (HOMO) and the lowest unoccupied molecular orbital (LUMO). The HOMO is outermost higher energy orbital containing electrons so it acts as an electron donor. The LUMO is the lowest energy orbital that has the room to accept electrons so it acts as an electron acceptor. The frontier molecular orbitals can offer a reasonable qualitative prediction of the excitation properties and the ability of electron transport [57, 58]. The HOMO and LUMO are also very popular quantum chemical parameters which determine the molecular reactivity. The energies of the HOMO and LUMO orbitals of the title compound are calculated using DFT/B3LYP method and shown in Fig. 3. The energies of HOMO and LUMO are negative, which indicates that the studied compound is stable [59]. In the title compound, the HOMO of π nature is delocalized over the phenyl ring PhI, C=O, C=C groups and LUMO in addition to this on the PhII ring. Accordingly, the HOMO-LUMO transition implies an electron density transfer from the phenyl ring PhI to the PhII ring through the propane group. For understanding various aspects of pharmacological sciences including drug design and the possible eco-toxicological characteristics of the drug molecules, several new chemical reactivity descriptors have been proposed. Conceptual DFT based descriptors have helped in many ways to understand the structure of the molecules and their reactivity by calculating the chemical potential, global hardness and electrophilicity. Using HOMO and LUMO orbital energies, the ionization energy and electron affinity can be expressed as: $I = -E_{\text{HOMO}}$, $A = -E_{\text{LUMO}}$, $\eta = (-E_{\text{HOMO}} + E_{\text{LUMO}})/2$ and $\mu = (E_{\text{HOMO}} + E_{\text{LUMO}})/2$ [60]. Parr *et al.* [61] proposed the global electrophilicity power of a ligand as $\omega = \mu^2/2\eta$. This index measures the stabilization in energy when the system acquired an additional electronic charge from the environment. Electrophilicity encompasses both the ability of an electrophile to acquire additional electronic charge and the resistance of the system to exchange electronic charge with the environment. It contains information about both electron transfer (chemical potential) and stability (hardness) and is a better descriptor of global chemical reactivity. The hardness η and chemical potential μ are given by the following relations: η

= $(I-A)/2$ and $\mu = -(I+A)/2$, where I and A are the first ionization potential and electron affinity of the chemical species [62]. For the title compound, $E_{\text{HOMO}} = -8.82$ eV, $E_{\text{LUMO}} = -6.23$ eV, energy gap = HOMO-LUMO = 2.59 eV, Ionization potential $I = 8.82$ eV, Electron affinity $A = 6.23$ eV, global hardness $\eta = 1.295$ eV, chemical potential $\mu = -7.525$ eV and global electrophilicity = $\mu^2/2\eta = 21.86$ eV. It is seen that the chemical potential of the title compound is negative and it means that the compound is stable. They do not decompose spontaneously into the elements they are made up of. The hardness signifies the resistance towards the deformation of electron cloud of chemical systems under small perturbation encountered during the chemical process. The principle of hardness works in chemistry and physics but it is not physically observable. Soft systems are large and highly polarizable, while hard systems are relatively small and much less polarizable.

4.5. Molecular Electrostatic Potential (MEP)

MEP is related to the electron density and is a very useful descriptor in understanding sites for electrophilic and nucleophilic reactions as well as hydrogen bonding interactions [63, 64]. The electrostatic potential $V(r)$ is also well suited for analyzing processes based on the "recognition" of one molecule by another, as in drug-receptor, and enzyme-substrate interactions, because it is through their potentials that the two species first "see" each other [65,66]. To predict reactive sites of electrophilic and nucleophilic attacks for the investigated molecule, MEP at the B3LYP level optimized geometry was calculated. The different values of the electrostatic potential at the MEP surface are represented by different colors: red, blue and green represent the regions of most negative, most positive and zero electrostatic potential respectively. The negative electrostatic potential corresponds to an attraction of the proton by the aggregate electron density in the molecule (shades of red), while the positive electrostatic potential corresponds to the repulsion of the proton by the atomic nuclei (shade of blue). The negative (red and yellow) regions of MEP were related to electrophilic reactivity and the positive (blue) regions to nucleophilic reactivity (Fig. 4). From the MEP it is evident that the negative charge covers the C=O group and the positive region is over the phenyl rings. The value of the electrostatic potential is largely responsible for the binding of a

substrate to its receptor binding sites since the receptor and the corresponding ligands recognize each other at their molecular surface [67, 68].

4.6. Geometrical parameters

The aromatic rings of the title compound are somewhat irregular and the spread of the C-C bond distance is 1.3892-1.4089Å (DFT), 1.3856-1.4044Å (XRD) for ring PhI and 1.3891-1.4061Å (DFT), 1.3790-1.4016Å (XRD) for ring PhII, which is similar to the spread reported by Smith et al., [69]. The C-Cl bond length 1.7549Å (DFT), 1.7379 Å (XRD) is in agreement with the C-Cl bond length given by Mariamma et al. [70]. The C-F bond length is reported as 1.3915Å [71], 1.3242Å [72], 1.3267 Å [32] and in the present case as 1.3462Å (DFT) and 1.3560Å (XRD). Chlorine and fluorine are highly electronegative and tries to obtain additional electron density. It attempts to draw it from the neighboring atoms which moves closer together in order to share the electrons more easily as a result. Due to this the bond angles C₂₂-C₂₄-C₂₅ and C₉-C₈-C₆ are found to be 121.0° and 122.1° in the present calculation, which is 120° for normal benzene. According to our calculations, at C₁₃ and C₁₄ positions, the bond angles are C₁₁-C₁₃-C₄ = 118.6, C₁₁-C₁₃-C₁₄ = 117.3, C₄-C₁₃-C₁₄ = 124.0° and C₁₅-C₁₄-O₃ = 120.9, C₁₅-C₁₄-C₁₃ = 119.3, C₁₃-C₁₄-O₃ = 119.8°, respectively and this shows the interaction between O₃ and H₁₂ atom. For the title compound, the C=O bond length is 1.2300Å (DFT). 1.2279Å (XRD) and C=C bond length is 1.3483Å (DFT), 1.3380Å (XRD) which are in agreement with the reported values [73, 74]. The discrepancies between the calculated geometrical parameters and XRD results are due to the fact that the comparison made between the experimental data, obtained from single crystal and calculated results are for isolated molecule in the gaseous phase.

5. Conclusion

In the present study, the structural geometrical parameters, vibrational wavenumbers and nonlinear optical properties of (*E*)-3-(4-chlorophenyl)-1-(4-fluorophenyl)prop-2-en-1-one have been studied using both the HF and DFT methods. The geometrical parameters obtained from XRD data are in agreement with the theoretical values (DFT). The complete vibrational assignments of wavenumbers have been made on the basis of potential energy distribution and found to be in good agreement with experimental values. The first order hyperpolarizability value implies that the title molecule may be

useful as a nonlinear optical material. Stability of the molecule arising from hyper-conjugative interaction and charge delocalization has been analyzed using NBO analysis. MEP, HOMO and LUMO analysis are also reported.

Acknowledgements

The authors would like to thank Dr.Hema Tresa Varghese, FMN College, Kollam, Kerala, India and University of Antwerp for providing computational facility.

References

- [1] C.B. Patil, S.K. Mahajan, S.A. Katti, *J. Pharm. Sci. Res.* 1 (2009) 11-22.
- [2] S.S. Mokle, M.A. Sayeed, K. Chopde, *Int. J. Chem. Sci.* 2 (2004) 96-101.
- [3] P.K. Pankaj, N.P. Bhanubhai, B. Anil, N.P. Jivani, *Der Pharm. Sinica* 2 (2011) 194-200.
- [4] G.S. Viana, M.A. Bandeira, F. Matos, *Phytomedicine* 10 (2003) 189-195.
- [5] L.M. Zhao, H.S. Jin, L.P. Sun, H.R. Piao, Z.S. Quan, *Bioorg. Med. Chem. Lett.* 15 (2005) 5027-5029.
- [6] S. Mukarami, M. Muramatsu, H. Aihara, S. Otomo, *Biochem. Pharmacol.* 42 (1991) 1447-1451.
- [7] M. Liu, P. Wilairat, L.M. Go, *J. Med. Chem.* 44 (2001) 4443-4452.
- [8] E. Francesco, G. Salvatore, M. Luigi, C. Massimo, *Phytochem.* 68 (2007) 939-953.
- [9] J.C. Onyilagna, B. Malhotra, M. Eldeer, G.H.N. Towers, *Can. J. Plant. Pathol.* 19 (1997) 133-137.
- [10] S.F. Nielsen, M. Chen, T.G. Theander, A. Kharazmi, S.B. Christensen, *Bioorg. Med. Chem. Lett.* 5 (1995) 449-452.
- [11] C.L. Miranda, G.L.M. Aponso, J.F. Stevens, M.L. Deinzer, D.R. Buhler, *J. Agric. Food Chem.* 48 (2000) 3876-3884
- [12] P.M.S. Kumar, S.K.G. Babu, D. Mukesh, *Chem. Pharm. Bull.* 55 (2007) 44-49.
- [13] M. Satyanarayana, P. Tiwari, K. Tripathi, A.K. Srivastava, R. Pratap, *Bioorg. Med. Chem.* 12 (2004) 883-889.
- [14] L. Barford, K. Kemp, A. Kharazmi, *Int. Immunopharmacol.* 2 (2002) 545-550.
- [15] H.H. Ko, L.T. Tsao, K.L. Yu, C.T. Liu, J.P. Wang, C.N. Lin, *Bioorg. Med. Chem.* 11(2003) 105-111.

- [16] A.M. Deshpande, N.P. Argade, A.A. Natu, *Bioorg. Med. Chem.* 7 (1999) 1237-1240.
- [17] S. Khatib, O. Nerya, R. Musa, M. Shmnel, S. Tamir, J. Vaya, *Bioorg. Med. Chem.* 13 (2005) 433-441.
- [18] F. Severi, S. Benvenuti, L. Costantino, G. Vampa, M. Melegari, L. Antolini, *Eur. J. Med. Chem.* 33 (1998) 859-866.
- [19] J. Cianci, J.B. Baell, B.L. Flynn, R.W. Gable, J.A. Mould, *Bioorg. Med. Chem. Lett.* 18 (2008) 2055-2061.
- [20] C.N. Lin, H.K. Hsieh, H.H. Ko, M.F. Hsu, H.C. Lin, *Drug. Dev. Res.* 53 (2001) 9-14.
- [21] G.M. Sheldrick, SHELXL-97 Program for the solution of crystal structures, University of Gottingen, Germany 1997.
- [22] Gaussian 09, Revision B.01, M.J. Frisch, G.W. Trucks, H.B. Schlegel, G.E. Scuseria, M.A. Robb, J.R. Cheeseman, G. Scalmani, V. Barone, B. Mennucci, G.A. Petersson, H. Nakatsuji, M. Caricato, X. Li, H.P. Hratchian, A.F. Izmaylov, J. Bloino, G. Zheng, J.L. Sonnenberg, M. Hada, M. Ehara, K. Toyota, R. Fukuda, J. Hasegawa, M. Ishida, T. Nakajima, Y. Honda, O. Kitao, H. Nakai, T. Vreven, J.A. Montgomery, J.E. Peralta, F. Ogliaro, M. Bearpark, J.J. Heyd, E. Brothers, K.N. Kudin, V.N. Staroverov, T. Keith, R. Kobayashi, J. Normand, K. Raghavachari, A. Rendell, J.C. Burant, S.S. Iyengar, J. Tomasi, M. Cossi, N. Rega, J.M. Millam, M. Klene, J.E. Knox, J.B. Cross, V. Bakken, C. Adamo, J. Jaramillo, R. Gomperts, R.E. Stratmann, O. Yazyev, A.J. Austin, R. Cammi, C. Pomelli, J.W. Ochterski, R.L. Martin, K. Morokuma, V.G. Zakrzewski, G.A. Voth, P. Salvador, J.J. Dannenberg, S. Dapprich, A.D. Daniels, O. Farkas, J.B. Foresman, J.V. Ortiz, J. Cioslowski, D.J. Fox, Gaussian, Inc., Wallingford CT, 2010.
- [23] J.B. Foresman, in: E. Frisch (Ed.), *Exploring Chemistry with Electronic Structure Methods: A Guide to Using Gaussian*, Pittsburg, PA, 1996.
- [24] R. Dennington, T. Keith, J. Millam, *Gaussview, Version 5*, Semichem Inc. Shawnee Mission KS, 2009.

- [25] J.M.L. Martin, C. Van Alsenoy, GAR2PED, A Program to obtain a potential energy distribution from a Gaussian archive record, University of Antwerp, Belgium (2007).
- [26] J. Coates in: R.A. Meyers, (Ed.) Interpretation of Infrared Spectra, A Practical approach, John Wiley and Sons Inc. Chichester 2000.
- [27] N.G.P. Roeges, A Guide to the Complete Interpretation of the Infrared spectra of organic structures, Wiley, New York 1994.
- [28] G. Varsanyi, Assignments of Vibrational Spectra of Seven Hundred Benzene Derivatives, Wiley, New York 1974.
- [29] C.Y. Panicker, K.R. Ambujakshan, H.T. Varghese, S. Mathew, S. Ganguli, A.K. Nanda, C. Van Alsenoy, *J. Raman Spectrosc.* 40 (2009) 527-536.
- [30] D. Philip, A. John, C.Y. Panicker, H.T. Varghese, *Spectrochim. Acta* 57A (2001) 1561-1566.
- [31] N. B. Colthup, L. H. Daly, S. E. Wiberly, Introduction to Infrared and Raman spectroscopy, Ed.3, Academic Press: Boston, 1990.
- [32] P.L. Anto, C.Y. Panicker, H.T. Varghese, D. Philip, O. Temiz-Arpaci, B.T. Gulbas, I. Yildiz, *Spectrochim. Acta* 67A (2007) 744-749.
- [33] C. Lee, W. Yang, R. G. Parr, *Phys. Rev.* 37B (1998) 785-789.
- [34] E. F. Mooney, *Spectrochim. Acta* 20 (1964) 1021-1032.
- [35] E. F. Mooney, *Spectrochim. Acta* 19 (1963) 877-887.
- [36] N. Sundaraganesan, C. Meganathan, B. D. Joshua, P. Mani, A. Jayaprakash, *Spectrochim. Acta* 71A (2008) 1134-1139.
- [37] P. Pazdera, H. Divisova, H. Havelsova, P. Borek, *Molecules* 5 (2000) 189-194.
- [38] P. Pazdera, H. Divisova, H. Havelsova, P. Borek, *Molecules* 5 (2000) 1166-1174.
- [39] H. T. Varghese, C. Y. Panicker, D. Philip, P. Pazdera, *Spectrochim. Acta* 67A (2007) 1055-1059.
- [40] W.O. George, P.S. McIntyre, *Infrared Spectroscopy* (1st edn), John Wiley and sons, Chichester, 1987.
- [41] M. A. Palafox, V. K. Rastogi, L. Mittal, *Int. J. Quantum Chem.* 94 (2003) 189-204.
- [42] M. Kurt, *J. Raman Spectrosc.* 40(1) (2009) 67-75.

- [43] R.M. Silverstein, G.C. Bassler, T.C. Morrill, *Spectrometric Identification of Organic Compounds*, 5th ed., John Wiley and Sons, Inc., Singapore, 1991.
- [44] M. Cinar, M. Karabacak, *Spectrochim. Acta* 104 (2013) 428-436.
- [45] V. Arjunan, A. Raj, S. Subramanian, S. Mohan, *Spectrochim. Acta* 110 (2013) 141-150.
- [46] G. Mariappan, N.S. Sundaraganesan, *Spectrochim. Acta* 110 (2013) 169-178.
- [47] G. Socrates, *Infrared Characteristic Group Frequencies*, John Wiley and Sons, New York 1981.
- [48] K. Felfoldi, M. Sutyinszky, N. Nagy and I. Palinko, *Synth. Commun.* 30 (2000) 1543-1553.
- [49] T. Joseph, H.T.Varghese, C.Y. Panicker, T. Thiemann, K. Viswanathan, C. Van Alsenoy, T.K. Manojkumar, *Spectrochim. Acta* 117 (2014) 413-421.
- [50] Y.R. Shen, *The Principles of Nonlinear Optics*, Wiley, New York, 1984.
- [51] P.V. Kolinsky, *Opt. Eng.* 31 (1992) 11676 - 11684.
- [52] D.F. Eaton, *Science* 25 (1991) 281-287.
- [53] D.A. Kleinman, *Phys. Rev.* 126 (1962) 1977-1979.
- [54] M. Adant, L. Dupuis, L. Bredas, *Int. J. Quantum. Chem.* 56 (2004) 497-507.
- [55] E.D. Glendening, A.E. Reed, J.E. Carpenter, F. Weinhold, NBO Version 3.1, Gaussian Inc., Pittsburgh, PA, 2003.
- [56] J. Choo, S. Kim, H. Joo, Y. Kwon, *J. Mol. Struct. (Theochem.)* 587 (2002) 1-8.
- [57] M. Belletete, J.F. Morin, M. Leclerc, G. Durocher, *J. Phys. Chem.* 109A (2005) 6953-6959.
- [58] D. Zhenminga, S. Hepinga, L. Yufanga, L. Dianshenga, L. Bob, *Spectrochim. Acta A* 78 (2011) 1143-1148.
- [59] S.W. Xia, X. Xu, Y.L. Sun, Y.L. Fan, Y.H. Fan, C.F. Bi, D.M. Zhang, L.R. Yang, *Chin. J. Struct. Chem.* 25 (2006) 197-203.
- [60] T.A. Koopmans, *Physica* 1 (1993) 104-113.
- [61] R.J. Parr, L.V. Szentpaly, S. Liu, *J. Am. Chem. Soc.* 121 (1999) 1922-1924.
- [62] R.J. Parr, R.G. Pearson, *J. Am. Chem. Soc.* 105 (1983) 7512-7516.
- [63] E. Scrocco, J. Tomasi, *Adv. Quantum. Chem.* 11 (1979) 115-121.
- [64] F.J. Luque, J.M. Lopez, M. Orozco, *Theor. Chem. Acc.* 103 (2000) 343-345.

- [65] P. Politzer, J.S. Murray, in: D.L. Beveridge, R. Lavery (Eds.), Theoretical Biochemistry and Molecular Biophysics: A Comprehensive Survey. Protein, vol. 2, Adenine Press, Schenectady, New York 1991.
- [66] E. Scrocco, J. Tomasi, *Curr. Chem.* 42 (1973) 95–170.
- [67] H. Kobinyi, G. Folkers, Y.C. Martin, 3D QSAR in Drug Design Vol. 3, Recent Advances, Kluwer Academic Publishers, 1998.
- [68] S. Moro, M. Bacilieri, C. Ferrari, G. Spalluto, *Curr. Drug Discovery Technol.* 2 (2005) 13-21.
- [69] G. Smith, D.E. Lynch, K.A. Byriel, C.H.L. Kennard, *Aust. J. Chem.* 48 (1995) 1133-1149.
- [70] K.C. Mariamma, H.T. Varghese, C.Y. Panicker, K. John, J. Vinsova, C. Van Alsenoy, *Spectrochim. Acta* 112 (2013) 161-168.
- [71] Y.S. Mary, K. Raju, T.E. Bolelli, I. Yildiz, H.I.S. Nogueira, C.M. Granadeiro, C. Van Alsenoy, *J. Mol. Struct.* 1012 (2012) 22-30.
- [72] Y.S. Mary, H.T. Varghese, C.Y. Panicker, T. Ertan, I. Yildiz, O. Temiz-Arpaci, *Spectrochim. Acta* 71 (2008) 566-571.
- [73] T. Rajamani, S. Muthu, *Solid State Sci.* 16 (2013) 90-101.
- [74] J.J. Nie, D.J. Xu, *Chinese Struct. J. Chem.* 21 (2002) 165-167.

Fig.1 FT-IR spectrum of (*E*)-3-(4-chlorophenyl)-1-(4-fluorophenyl)prop-2-en-1-one

Fig.2 Optimized geometry (b3LYP) of (*E*)-3-(4-chlorophenyl)-1-(4-fluorophenyl)prop-2-en-1-one

Fig.3 HOMO and LUMO plots of (*E*)-3-(4-chlorophenyl)-1-(4-fluorophenyl)prop-2-en-1-one

Fig.4 MEP plot of (*E*)-3-(4-chlorophenyl)-1-(4-fluorophenyl)prop-2-en-1-one

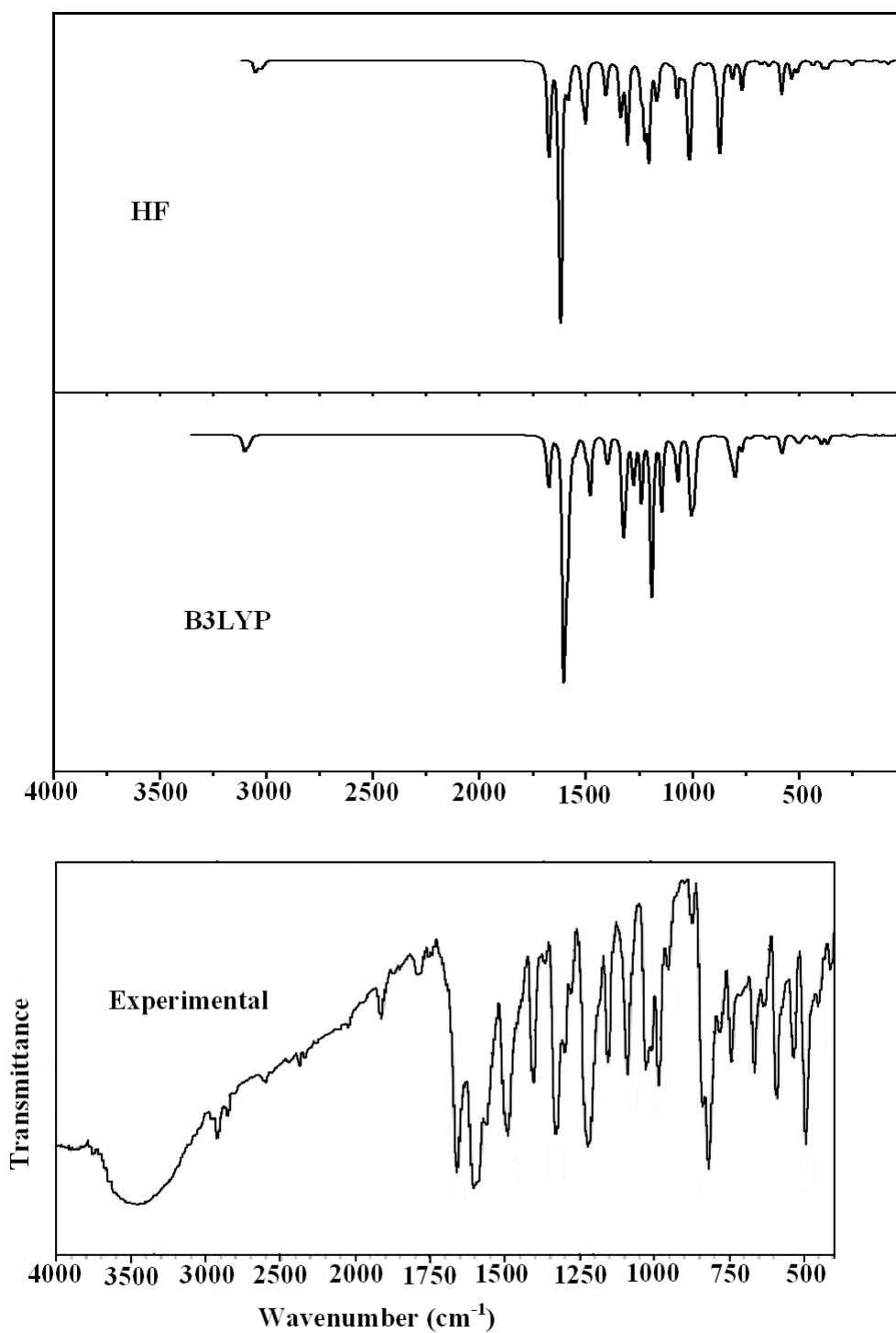


Fig.1 FT-IR spectrum of (E)-3-(4-Chlorophenyl)-1-(4-fluorophenyl)prop-2-en-1-one

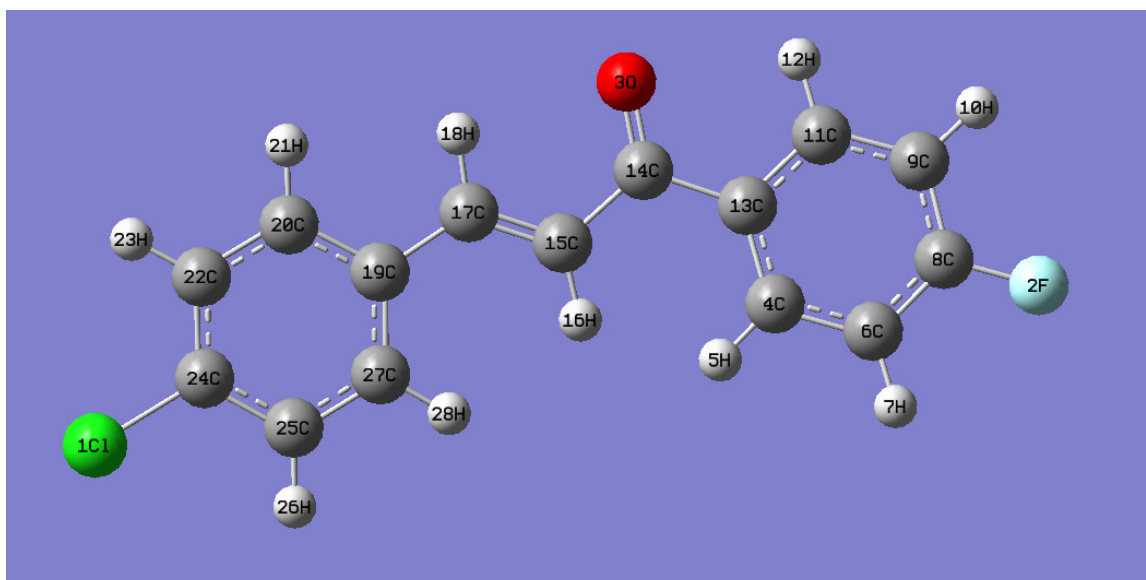
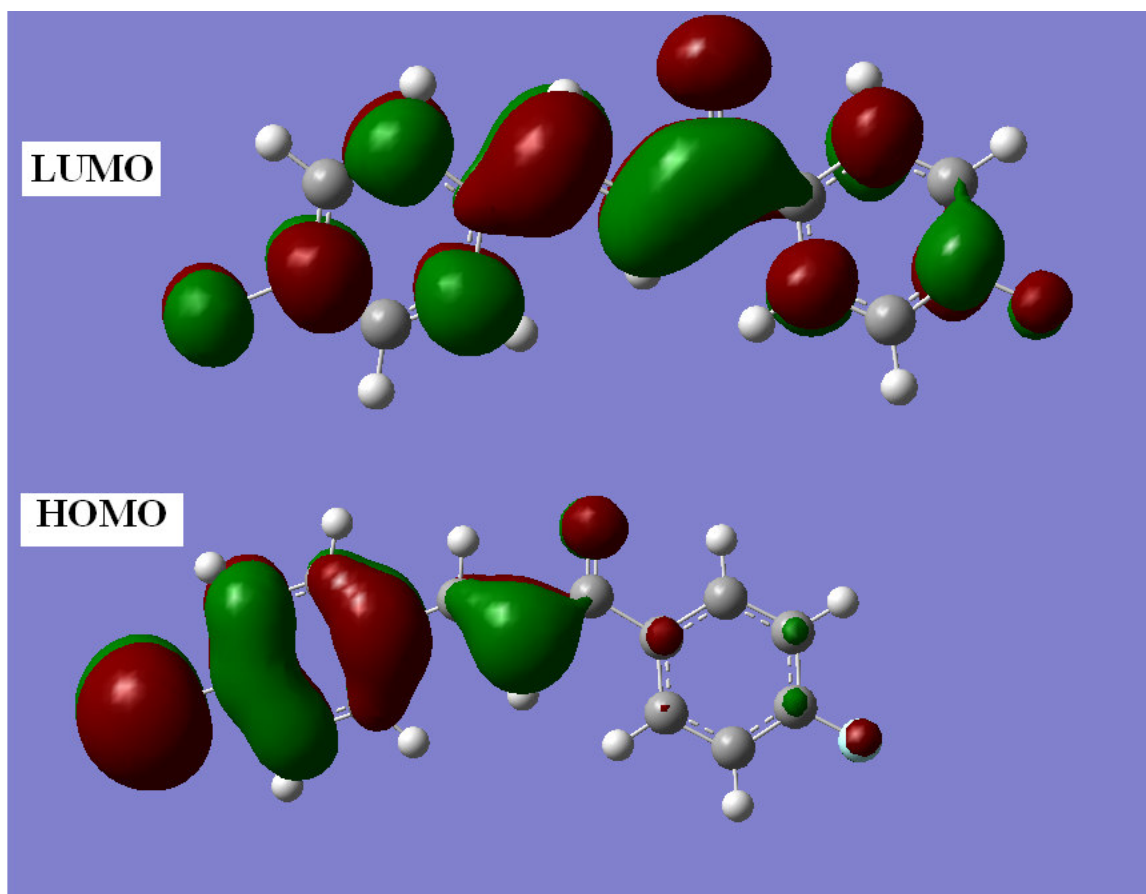


Fig.2 Optimized geometry (b3LYP) of
(E)-3-(4-chlorophenyl)-1-(4-fluorophenyl)prop-2-en-1-one

ACCEPTED MA



**Fig.3 HOMO and LUMO plots of
(*E*)-3-(4-chlorophenyl)-1-(4-fluorophenyl)prop-2-en-1-one**

ACCEPTED

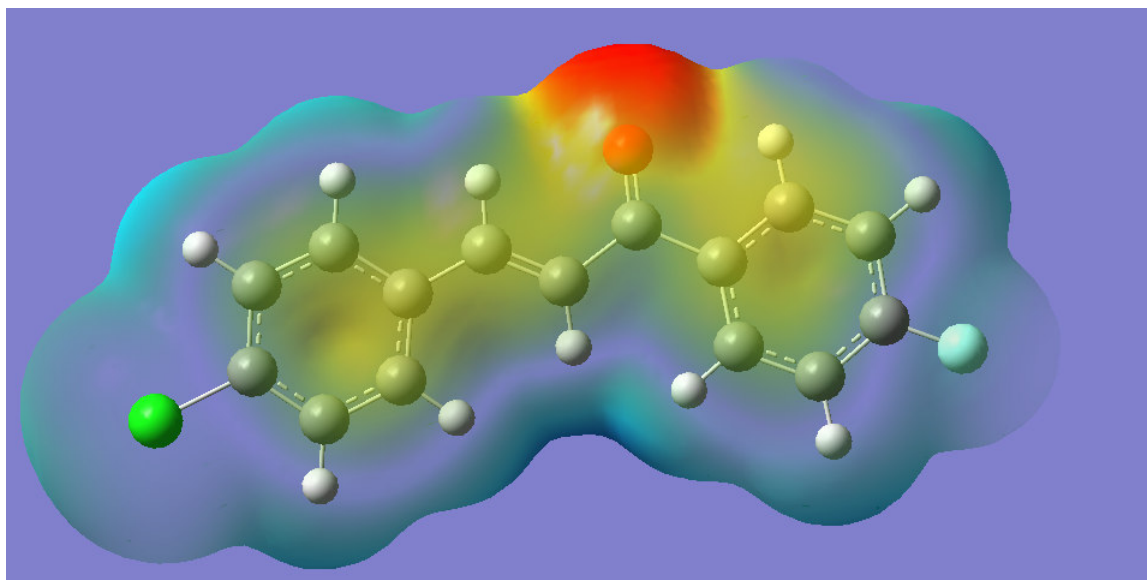


Fig.4 MEP plot of
(E)-3-(4-chlorophenyl)-1-(4-fluorophenyl)prop-2-en-1-one

ACCEPTED MA

Table 1. Vibrational assignments of (*E*)-3-(4-chlorophenyl)-1-(4-fluorophenyl)prop-2-en-1-one

HF/6-31G(6D,7F)		B3LYP/6-31G(6D,7F)		IR	Assignments ^a
ν	IR _I	ν	IR _I	ν	-
3056	3.78	3110	4.76	3156	ν CHII(96)
3054	10.40	3107	14.59	-	ν CHII(76), ν CH(17)
3048	1.63	3103	3.43	-	ν CHI(96)
3045	2.36	3101	4.50	-	ν CHI(93)
3044	3.26	3097	1.63	-	ν CHII(64), ν CH(26)
3041	0.74	3096	6.35	-	ν CHII(88)
3030	11.02	3085	11.22	-	ν CHII(22), ν CH(44), ν CHI(20)
3022	2.81	3079	1.18	-	ν CHI(68), ν CH(21)
3012	6.52	3073	5.65	-	ν CHI(98)
2999	0.10	3053	0.67	-	ν CH(98)
1674	197.65	1676	113.61	1665	ν C=O(55), ν C=C(15)
1621	307.98	1604	370.64	1605	ν C=O(12), ν C=C(50)
1618	215.21	1596	84.68	-	ν PhII(46), ν PhI(12)
1609	7.02	1584	176.12	-	ν PhI(41), ν PhII(21)
1588	24.42	1573	8.03	-	ν PhII(63), δ CHI(12)
1579	34.65	1552	29.89	1551	ν PhI(68), δ CHII(16)
1518	36.11	1497	29.96	1496	ν PhII(45), δ CHI(10)
1503	109.46	1480	91.83	-	ν PhI(42), δ CHII(18)
1407	64.27	1400	52.98	1402	ν PhII(48), ν PhI(12)
1402	6.88	1395	12.11	-	ν PhII(14), ν PhI(43)
1343	3.07	1324	144.54	1330	δ CH(42), ν PhII(21)
1336	109.39	1315	83.70	-	ν PhI(19), δ CH(42)
1311	5.09	1305	1.00	-	ν PhII(81), δ CHI(10)
1306	140.45	1286	1.41	-	ν PhI(27), δ CHI(57)
1241	40.64	1276	88.37	1279	ν PhI(48), ν CC(14)
1225	87.95	1272	2.44	-	δ CHII(72)

1218	34.62	1239	104.80	-	ν CF(51), δ CHII(26)
1204	147.59	1195	22.47	1202	ν CC(35), δ CH(17), ν PhI(17)
1192	0.59	1191	252.74	-	ν CC(44), δ CHI(20)
1178	6.37	1169	3.02	-	ν PhI(12), δ CHI(81)
1166	75.96	1144	118.32	1148	δ CHII(73)
1107	2.19	1099	5.05	1098	ν PhI(26), δ CHI(54)
1098	2.89	1088	7.95	-	ν PhII(24), δ CHII(61)
1073	55.41	1070	89.35	-	ν PhI(15), δ CHI(45)
1051	18.79	1007	132.35	1007	δ CHII(38), ν CC(39)
1044	7.59	999	22.98	-	γ CH(53), τ C=C(32)
1036	0.62	992	32.17	-	δ PhII(51), ν PhII(21)
1025	27.74	990	43.82	989	δ PhI(62), ν PhI(19)
1019	45.27	954	0.27	952	γ CHII(88)
1014	5.05	928	0.63	-	γ CHI(82), τ PhI(11)
1013	65.18	923	0.38	-	γ CHI(86)
1011	73.47	909	0.78	-	γ CHII(84)
942	5.91	874	1.67	878	δ C=C(10), δ CH(12), ν PhI(41)
894	13.21	856	0.18	858	γ CH(50), γ C=O(12)
881	8.27	827	11.88	820	γ CHII(51), γ CHI(22)
875	58.67	817	20.18	820	δ PhII(14), ν PhII(40)
871	91.91	804	37.82	806	γ CHI(66), γ CHII(11)
863	35.07	801	31.70	-	γ CHI(78)
812	24.88	794	28.66	790	γ CHII(78)
770	17.06	767	25.07	-	δ PhI(17), δ C=O(34), δ PhII(10)
765	35.17	727	5.65	730	τ PhII(27), τ PhI(16), τ C=O(14)
736	0.61	686	0.11	-	τ PhII(24), τ PhI(45)
676	6.42	650	3.40	-	τ PhII(42), τ PhI(16), γ C=O(10)

644	3.01	648	4.39	645	$\delta\text{PhI}(29)$, $\nu\text{CCl}(35)$
640	3.40	623	0.66	-	$\delta\text{PhI}(75)$
639	2.63	622	2.32	615	$\delta\text{PhII}(72)$
581	48.95	581	42.42	586	$\delta\text{PhII}(32)$, $\gamma\text{C=O}(38)$
534	27.33	513	9.08	515	$\delta\text{C=O}(28)$, $\delta\text{CF}(16)$, $\delta\text{CC}(17)$
511	17.29	497	12.91	-	$\tau\text{PhII}(21)$, $\gamma\text{CF}(20)$, $\tau\text{PhI}(15)$, $\gamma\text{CCl}(11)$, $\gamma\text{CC}(18)$
501	4.09	485	3.00	482	$\delta\text{PhI}(24)$, $\gamma\text{CCl}(17)$, $\gamma\text{CF}(15)$, $\tau\text{PhII}(15)$, $\gamma\text{CC}(14)$
435	7.77	440	7.07	450	$\delta\text{CF}(15)$, $\delta\text{CCl}(14)$, $\delta\text{CC}(18)$, $\delta\text{PhII}(12)$
428	0.60	407	0.56	409	$\tau\text{PhII}(80)$
421	0.08	402	0.08	-	$\tau\text{PhI}(80)$
387	15.70	396	16.06	-	$\delta\text{PhII}(11)$, $\delta\text{CF}(45)$
367	11.85	366	15.24	-	$\delta\text{PhII}(19)$, $\delta\text{CF}(12)$, $\delta\text{PhI}(11)$, $\delta\text{CC}(10)$
349	0.90	339	0.23	-	$\tau\text{PhI}(30)$, $\gamma\text{CCl}(30)$
314	1.72	315	0.99	-	$\delta\text{CCl}(35)$, $\delta\text{C=O}(14)$
299	1.25	297	0.11	-	$\gamma\text{CC}(30)$, $\tau\text{PhII}(33)$
249	6.50	254	5.35	-	$\delta\text{C=C}(12)$, $\delta\text{CC}(28)$,
					$\delta\text{CCl}(31)$
181	0.38	180	0.19	-	$\delta\text{C=C}(19)$, $\delta\text{PhI}(16)$,
					$\delta\text{CC}(34)$
178	1.22	171	0.27	-	$\tau\text{PhI}(26)$, $\gamma\text{CCl}(16)$,
					$\tau\text{C=O}(12)$
163	2.09	158	1.65	-	$\delta\text{CC}(36)$, $\delta\text{C=O}(11)$,
					$\tau\text{PhII}(11)$
114	2.99	121	1.17	-	$\tau\text{PhII}(33)$, $\tau\text{C=O}(16)$,
					$\delta\text{CC}(11)$
81	4.98	83	2.54	-	$\tau\text{CC}(36)$, $\gamma\text{CC}(13)$, $\tau\text{C=C}(12)$
60	0.87	58	1.00	-	$\tau\text{PhI}(28)$, $\tau\text{C=O}(17)$, $\gamma\text{CC}(13)$

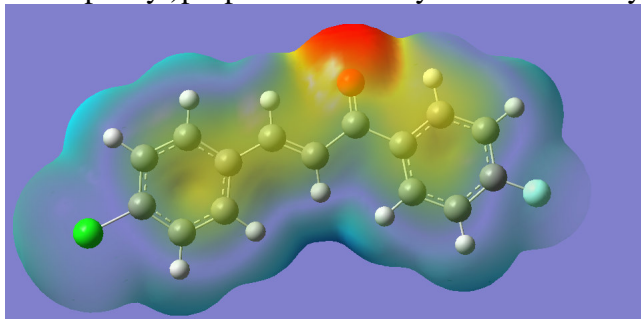
40	0.47	41	0.11	-	$\delta\text{C}=\text{C}(27)$, $\delta\text{C}=\text{O}(15)$, $\delta\text{CC}(10)$
28	0.14	22	0.02	-	$\tau\text{CC}(50)$, $\tau\text{C}=\text{O}(10)$
13	0.03	18	0.02	-	$\tau\text{CC}(54)$, $\tau\text{C}=\text{O}(20)$

^a ν -stretching; δ -in-plane deformation; γ -out-of-plane deformation; τ -torsion; PhI-phenyl ring attached with chlorine; PhII-phenyl ring attached with fluorine; IRI-IR intensity; potential energy distribution is given in brackets in the assignment column.

ACCEPTED MANUSCRIPT

Graphical abstract

Title of the paper: Molecular structure, FT-IR, first order hyperpolarizability, NBO analysis, HOMO and LUMO, MEP analysis of (*E*)-3-(4-chlorophenyl)-1-(4-fluorophenyl)prop-2-en-1-one by HF and density functional methods



ACCEPTED MANUSCRIPT

Highlights

- * IR, XRD and NBO analysis were reported.
- * The wavenumbers are calculated theoretically using Gaussian09 software.
- * The wavenumbers are assigned using PED analysis.
- * The geometrical parameters are in agreement with XRD data.

ACCEPTED MANUSCRIPT